Eur Radiol (2003) 13:2365–2371
DOI 10.1007/s00330-003-1878-8

Sebastian Ley
Hans-Ulrich Kauczor
Claus Peter Heussel
Thorsten Kramm
Eckhard Mayer
Manfred Thelen
Karl-Friedrich Kreitner

Value of contrast-enhanced MR angiography and helical CT angiography in chronic thromboembolic pulmonary hypertension

Received: 1 July 2002
Revised: 26 November 2002
Accepted: 3 February 2003
Published online: 24 April 2003

S. Ley (✉) · H.-U. Kauczor
C. P. Heussel · M. Thelen · K.-F. Kreitner
Department of Radiology,
Johannes Gutenberg University Mainz,
Langenbeckstrasse 1, 55131 Mainz,
Germany
e-mail: ley@gmx.de
Tel.: +49-6131-173663
Fax: +49-6131-176633

T. Kramm · E. Mayer
Department of Cardiac,
Thoracic and Vascular Surgery,
Johannes Gutenberg University Mainz,
Langenbeckstrasse 1,
55131 Mainz, Germany

Abstract The aim of this study was to evaluate the diagnostic value of contrast-enhanced MR angiography (ce MRA) and helical CT angiography (CTA) of the pulmonary arteries in the preoperative workup of patients with chronic thromboembolic pulmonary hypertension (CTEPH). The ce MRA and CTA studies of 32 patients were included in this retrospective evaluation. Image quality was scored by two independent blinded observers. Data sets were assessed for number of patent segmental, subsegmental arteries, and number of vascular segments with thrombotic wall thickening, intraluminal webs, and abnormal proximal to distal tapering. Image quality for MRA/CTA was scored excellent in 16 of 16, good in 11 of 14, moderate in 2 of 5, and poor in no examinations. The MRA/CTA showed 357 of 366 patent segmental and 627 of 834 patent subsegmental arteries. CTA was superior to MRA in visualization of thrombotic wall thickening (339 vs 164) and of intraluminal webs (257 vs 162). Abnormal proximal to distal tapering was better assessed by MRA than CTA (189 vs 16). In joint assessment of direct and indirect signs, MRA and CTA were equally effective (353 vs 355). MRA and CTA are equally effective in the detection of segmental occlusions of the pulmonary arteries in CTEPH. CTA is superior for the depiction of patent subsegmental arteries, of intraluminal webs, and for the direct demonstration of thrombotic wall thickening.

Keywords Contrast-enhanced MR angiography · Helical CT angiography · Chronic thromboembolic pulmonary hypertension · Pulmonary arteries

Introduction

Chronic thromboembolic pulmonary hypertension (CTEPH) is a rare disease entity. Only 1–5% of patients with acute pulmonary emboli develop a chronic progression resulting in a decrease of pulmonary arterial vessel diameter with a consecutive increase of pulmonary arterial pressure [1, 2]. The thromboembolic material and its breakdown products are incorporated into the vessel wall resulting in thrombotic wall thickening and obliteration of the pulmonary arterial vasculature. Additionally, recanalization can occur resulting in a mixed picture of vascular stenosis, intraluminal webs, and abnormal proximal to distal tapering of vessel diameter. Increased vascular pressure can be compensated for a long time, but after occlusion of approximately 60% of the pulmonary arterial vascular bed the mean pulmonary arterial pressure (MPAP) rises [3]. This finally leads to right heart failure. An increase of MPAP over 30–40 mm Hg is associated with a 5-year survival rate of only 30%. After incorporation of the thrombotic material into the vessel wall the disease can only be cured by surgery: pulmonary thromboendarterectomy (PTE) is advised [2].

Technically, PTE can only be performed if the extent of vascular involvement is located proximal to the segmental arteries; therefore, preoperative workup has to

comprise a visualization of the occlusive thromboembolic material to determine surgical eligibility including determination of the proximal beginning of the wall thickening due to incorporated thromboembolic material [4].

Until recently, selective digital subtraction angiography (DSA) combined with right heart catheterization was considered the gold standard for evaluating the disease and for assessment of surgical resectability. Besides a clear visualization of the pulmonary vasculature, hemodynamic parameters can be obtained [5]. The diagnostic criteria in angiography are: visualization of bands and intraluminal webs; abnormal proximal to distal tapering; and vessel cutoffs. Over recent years, helical CT angiography (CTA) has become more and more accepted in the diagnosis of CTEPH as it enables non-invasive and fast visualization of the pulmonary vasculature [6]. Furthermore, it provides clear delineation of the central beginning of the organized thromboembolic material which is difficult to detect by DSA [7]. The implementation of high-performance gradient systems decisively improved the quality of contrast-enhanced magnetic resonance angiography (ce MRA); therefore, it can be used in the preoperative workup of CTEPH as well [8]. Hemodynamic parameters of the right ventricle and blood flow velocities in the pulmonary arteries can also be assessed by MRI [9, 10]. This combination makes it a promising complementary tool in assessment of CTEPH.

The goal of this study was to compare the value of CTA and ce MRA in the preoperative evaluation of patients with CTEPH. The evaluation focuses on the visualization of patent pulmonary arterial vessels branches, thrombotic wall thickening, abnormal proximal to distal tapering, and intraluminal webs. In addition, both modalities were compared for the assessment of surgical resectability.

Materials and methods

Thirty-two consecutive patients (11 women, 21 men) with a mean age of 54 years (range 22–72 years) for normal preoperative workup were included in this retrospective study. The median time interval between MRA and CTA was 2 days (±39 days) including all patients but three. In two patients MRA was 1 year (359 and 358 days, respectively) prior to CTA. In 1 patient CTA was performed 4 years before MRA. During these time intervals, there was no clinical evidence of further thromboembolic events in the patients. The diagnosis of CTEPH was proven by DSA and surgery in all cases. As MRI, CT, and pulmonary DSA are a substantial part of the diagnostic workup in these patients, formal approval was not required by the local ethics committee; however, informed consent was obtained before all examinations.

CTA was done using a single-slice PQ 6000 scanner (Picker International, Cleveland, Ohio). The acquisition parameters were as follows: collimation 3 mm; pitch 2; increment 2 mm; and caudo-cranial scan direction. The field of view (FOV) was zoomed onto the mediastinum with a square dimension of approximately 200 mm. During a single breath hold the whole chest was examined (32 s). Oxygen supply was necessary in very dyspneic patients. We administered 120 ml of a non-ionic contrast medium (Iopromide 300, Ultravist, Schering, Berlin, Germany) in an antecubital vein via a 20-G needle with a flow rate of 3 ml/s followed by a saline flush of 50 ml with 3 ml/s using a power injector (XD 5500, Ulrich GmbH, Ulm, Germany). The delay between contrast agent administration and the start of the spiral scan was constantly 15 s. There was no repetition of contrast media application.

MR imaging was performed on a 1.5-T system (gradient field strength 25 mT/m, minimal rise time of 300 μs; Magnetom Vision, Siemens, Erlangen, Germany) using a phased-array body coil. For MRA, we used a non-ECG-triggered, radio-frequency-spoiled 3D fast low-angle shot (FLASH) sequence that was acquired in a coronal orientation (TR/TE=4.6 ms/1.8 ms, flip angle 30°, FOV 400 mm, matrix 512×512 pixel). In phase-encoding direction the rectangular FOV was adapted to the size of the patient and the matrix was reduced to 52%. The slab thickness of the 3D volume was 112 mm. Thirty-two partitions were acquired. After slice interpolation, the voxel size was 1.5×0.78×1.8 mm^3. Depending on the rectangular FOV, the acquisition time ranged between 23 and 27 s; thus, the examinations could be done in a single breath hold.

Each data set was enhanced by a standard dose of 20 ml Gd-DTPA (Schering, Berlin, Germany) injected with a flow of 2 ml/s followed by 20 ml saline flush in an antecubital vein via a 20-G needle using a MR compatible power injector (Spectris, Medrad, Pittsburgh, Pa.). The mean body weight of patients was 72 kg (range 49–98 kg) resulting in a contrast medium dosage of 0.14±0.02 mmol/kg body weight. In all cases there was only one injection of contrast media necessary for a diagnostically sufficient data set.

To optimize contrast agent timing, the individual circulation time was determined using a bolus of 2 ml (flow 2 ml/s) of Gd-DTPA followed by 20 ml saline flush (flow 2 ml/s). A 2D FLASH sequence with a temporal resolution of 1 s, planned axially at the level of the pulmonary trunk, was acquired. To calculate the time delay (T_D) the following equation was used: $T_D=T_K-T_{AC/2}+4$ s (T_K time interval between start of 2D FLASH and contrast media seen in the pulmonary trunk / T_{AC} acquisition time of 3D sequence) [11, 12].

An additional oxygen supply was necessary in three severely dyspneic patients.

Image evaluation

CT image analysis was done on a separate workstation (MagicView, Siemens, Erlangen, Germany), using axial source images (Fig. 1a) and interactive multiplanar reformations (MPR) in a soft tissue window setting adapted to the degree of vascular opacification. Image quality was subjectively ranked using a four-point score (1=excellent, 2=good, 3=moderate, 4=poor) comprising opacification of pulmonary vessels, and artifacts due to respiratory and cardiac motion. The MR image analysis was done using source images, maximum intensity projections (MIP; Fig. 2), and interactive MPR (Fig. 1b). The quality of images was subjectively ranked using the four-point score (see above). Criteria for scoring were enhancement of pulmonary vasculature, folding artifacts, and artifacts due to respiratory or cardiac motion.

The pulmonary vasculature was divided into two levels following the surgical classification (pulmonary trunk, main, lobar, and segmental arteries vs subsegmental level). The number of opacified pulmonary segments were counted. The images were assessed for morphologic changes such as thrombotic wall thickening, abnormal proximal to distal tapering, and intraluminal webs [13].

For comparison with the intra-operative situs, we compared imaging findings with surgical reports where the central beginning of the occlusive thromboembolic material was described in detail. These reports were only available after evaluation of the imaging modalities.

Data management and descriptive statistics were done using Microsoft Excel 2000 (Microsoft, Redmond, Wash.).

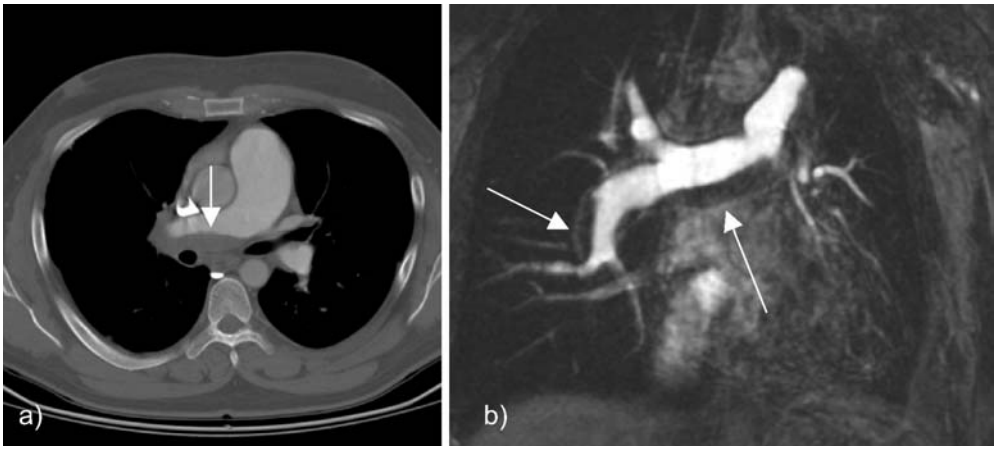

Fig. 1 **a** Axial computed tomography angiography (CTA) showing thromboembolic material incorporated into the vessel wall (*arrow*). **b** Multiplanar reconstruction of an MR angiogram showing centrally located thromboembolic material (*arrows*)

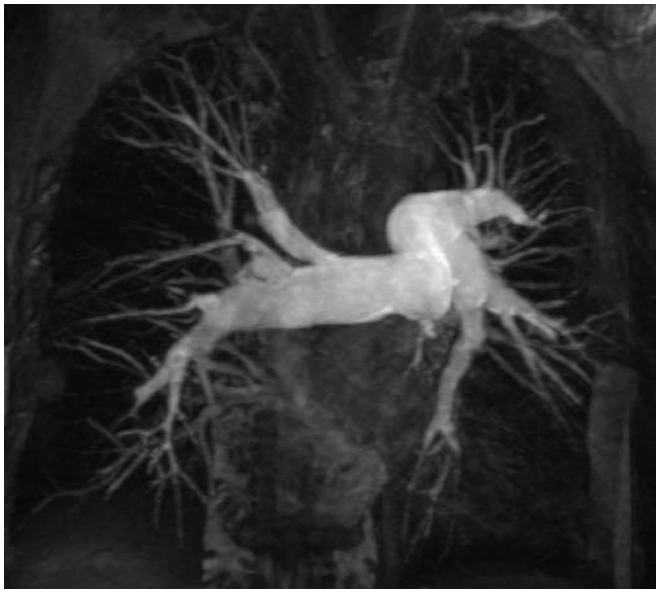

Fig. 2 An MR angiogram (MRA) of the pulmonary vasculature in a maximum intensity projection

Table 1 Number of investigations rated with the given image quality of CT angiography (*CTA*) and contrast-enhanced MR angiography (*ce MRA*)

Image quality score	CTA	ce MRA
Excellent (1)	16	16
Good (2)	11	14
Moderate (3)	5	2
Poor (4)	0	0

Table 2 Number of detected patent segmental and subsegmental pulmonary arteries in CTA and ce MRA

Patent arteries	CTA	ce MRA
Lobar/segmental level	357	366
Subsegmental level	834	627

Table 3 Absolute numbers of morphologic changes found in CTA and ce MRA

Morphologic evaluation	CTA	ce MRA
Thrombotic wall thickening	339	164
Intraluminal webs	257	162
Proximal to distal tapering	16	189
Wall thickening and tapering	355	353

Results

In 16 cases image quality was rated excellent on ce MRA and CTA. A good score was achieved by ce MRA in 14 and by CTA in 11 cases. Moderate scores were assigned in 2 (ce MRA) and in 5 (CTA) cases, respectively. No examination was of poor image quality (Table 1).

With respect to patent lobar and segmental arteries, ce MRA revealed a slightly higher number (366) than CTA (357). Patent subsegmental pulmonary arteries were visualized by CTA 834 and by ce MRA 627 times (Table 2).

Morphologic evaluation of pulmonary arterial vasculature revealed that thrombotic wall thickening was better visualized by CTA (339 vascular segments) than by use of ce MRA (164 vascular segments). Intraluminal webs were detected by CTA in 257 cases, and by MRA in 162 cases. Abnormal proximal to distal tapering of vessels was better detected on MR angiograms compared with CT angiograms (189 vs 16 times, respectively).

Summarizing all morphologic findings (direct visualization of thrombotic wall thickening and proximal to distal tapering), the "performance" of CTA and MRA was comparable (353 ce MRA vs 355 CTA; Table 3).

Both imaging modalities revealed technical operability that was confirmed by subsequent surgery. Compared with the intra-operative situs, ce MRA and CTA correctly predicted the proximal beginning of the thromboembolic material in the pulmonary arteries in all cases.

Discussion

We compared ce MRA and helical CTA for characterization of CTEPH, and to assess technical operability of patients with proven CTEPH. Image quality was diagnostically sufficient in all cases. The number of detected patent lobar pulmonary arteries were comparable at MRA and CTA. CTA was superior to MRA regarding visualization of subsegmental arteries. Different vascular abnormalities were assessed by the two modalities in different ways. While CTA is superior in direct visualization of thrombotic material, MRA enables better visualization of indirect signs of vascular changes such as abnormal tapering of vessels (Fig. 3).

CTEPH is a rare complication of acute pulmonary embolism with an incorporation of the thromboembolic material into the vessel wall with a consecutive narrowing of pulmonary arteries [14]. Surgical PTE is the only possible treatment to decrease pulmonary arterial pressure and resistance. After diagnosing CTEPH, the main preoperative task is to define its technical operability.

Pulmonary angiography in DSA technique, referred to as the gold standard in the diagnosis of pulmonary embolism [5], may not be accurate enough in detection of proximal clots [15, 16, 17], which is crucial in the assessment of technical operability.

Besides their non-invasiveness, it was shown in acute and chronic thromboembolism [6, 13] that an additional advantage of MRI and CT in comparison with DSA is the superior detection of non-occlusive emboli due to the lack of superimposition.

CT has shown its high potential for diagnosing CTEPH in several studies [6, 18, 19, 20]. In our study, CT scanning parameters were optimized as slice thickness was 3 mm with an increment of 2 mm. Furthermore, the standard field of view was targeted to the mediastinum, resulting in an in-plane resolution of 0.4×0.4 mm^2. MPR is possible especially when helical data are reconstructed using overlapping slices. An overlap of 30% was used in this study and the resulting detail resolution and image quality was high enough for evaluation of the pulmonary vasculature down to the subsegmental level by MPR. The higher in-plane resolution of CTA vs ce MRA was responsible for the higher number of detected patent subsegmental arteries and the detection of small intraluminal or mural thrombi, referred to as webs. It was shown that these signs were better assessed by CTA than by ce MRA.

Due to technical improvement, ce MRA has been shown to be of value in the diagnosis of pulmonary embolism. This has been shown mainly in the detection of acute pulmonary embolism with sensitivity ranging from 68 to 87% and specificity ranging from 97 to 99.7% [21, 22, 23]. Although these results are not directly applicable to CTEPH, it demonstrates the high quality of ce MRA in comparison with DSA. To our knowledge, there is only one state-of-the-art study that compared selective DSA with ce MRA for preoperative workup of CTEPH patients [8], but none that compared CTA and MRA. Kreitner et al. [8] found a sensitivity of ce MRA of 100% compared with DSA up to the level of the lobar arteries. For the subsegmental level a sensitivity of 87% was achieved.

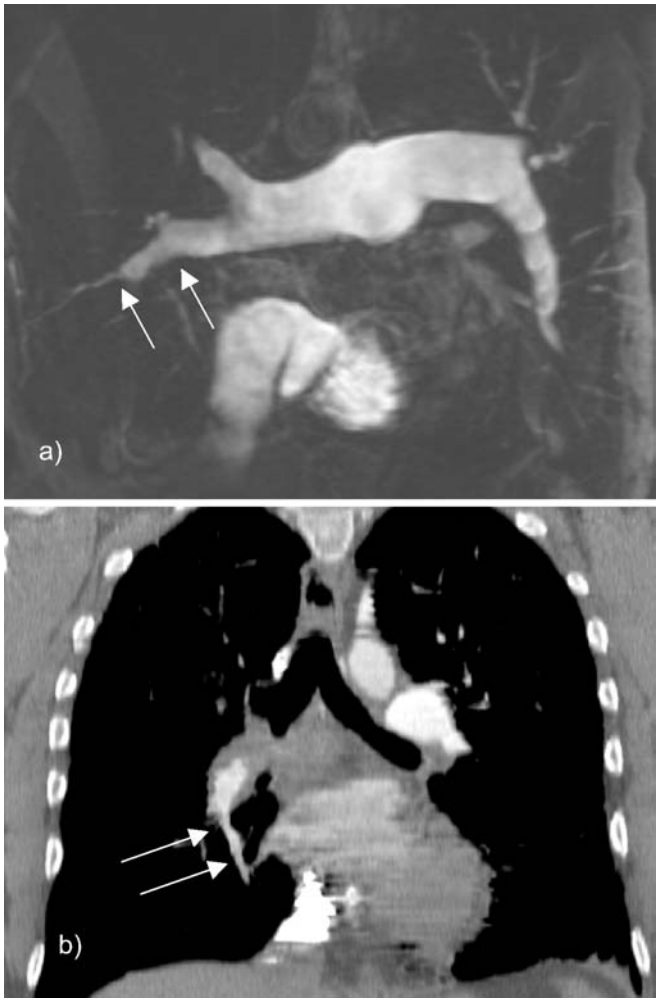

Fig. 3 Demonstration of abnormal proximal to distal tapering in multiplanar reformation (MPR) mode from **a** MRA and **b** CTA (*arrows*)

To enable a spatial resolution of 1.58×0.78×1.8 mm^3 in a breath hold, the lung volume coverage was reduced to 112 mm focused onto the central portion of the lung. This reduced the number of potentially visible subsegmental vessels; however, as surgical intervention is only possible if the major thromboembolic deposits are proximal to the segmental arteries [4], the reduced visibility of subsegmental arteries does not affect the decision for technical operability nor assessment of disease. For a precise evaluation of the pulmonary vasculature in MRA, it is necessary to analyze the source images and to use interactive MPR. Due to non-isotropic voxel size, the visualization of oblique vessels was not sufficient using double oblique MPR.

As contrast of the embolic material to the surrounding lung parenchyma is low in ce MRA, direct visualization of thromboembolic material was only moderate when compared with CT (339 vs 164 times), but the indirect sign of abnormal proximal to distal tapering was more often recognized (189 vs 16 times). This is due to the coronal acquisition enabling a very good assessment of abrupt caliber changes particularly at vessel bifurcations [8]. Taking together the vascular changes, the diagnostic value for assessing and defining technical operability is very similar with both modalities.

The lack of ECG trigger in ce MRA reduced the quality of vessel delineation near to the heart and especially subsegmental arteries of the lingula in our study. The ECG triggering would lead to an increase of acquisition time and would prevent breath-hold scanning.

To improve quality of ce MRA it is necessary to use latest MR scanner technology; however, even with use of high-end gradient systems, this can only be realized at the expense of a reduced spatial resolution. On a high-performance gradient system Goyen et al. [24] reduced the acquisition time for the pulmonary arterial tree down to 4 s. The pulmonary arterial tree was visible to the subsegmental level.

In our study image quality was assessed by visual criteria. The score was influenced by the breath-hold capabilities of the patient and additionally by folding artifacts in MR. Although both examinations had similar acquisition times (MRA 23–27 s vs CTA 32 s), this difference had a noticeable effect on image quality. There were only two MRA studies rated moderate due to the presence of folding artifacts, whereas five CT studies were considered to be moderate due to respiratory motion. In this context the principle differences between CT and MR have to be noted. As CT generally is less susceptible to motion artifacts due to the caudo-cranial scan direction, this observation reflects that an acquisition time of 32 s is too long for patients with severe dyspnea.

For MRA we used an asymmetric but linear k-space filling strategy, before calculation of images was done; thus, if there is any motion at any point the whole series gets worse [25]. Another effect onto image quality was related to contrast agent timing and/or superimpositions of other vascular territories, e.g., pulmonary veins and ascending aorta. The individual determination of circulation time was responsible for the slightly better image quality of MRA in comparison with CTA. If the contrast agent bolus is timed well and of a sharp geometry, only the pulmonary arterial phase is acquired without much venous overlay; however, as the passage time through the pulmonary arteries and veins needs only 3–5 s, it is not possible using this sequence to acquire images without any venous overlay [24]. In CTA there is continuous data acquisition and therefore the contrast agent will be in the lower pulmonary arteries by start of the scan. As the scanner is acquiring data of the hilar region after approximately 15 s, there is always some venous and aortic overlay.

Perspective

Some of the drawbacks of helical CT have already been overcome by introduction of multislice CT. Here it is possible to cover the entire chest of a patient with 1-mm slices within a single breath hold. Significant increase in spatial resolution in z-axis is followed by a significant increase in detection rate of subsegmental arteries [26]. These thin slices are comparable to high-resolution CT examinations making a direct evaluation of changes in the lung parenchyma possible [27], i.e., pleural based, wedge-shaped fibrosis, and mosaic perfusion [7]. Also functional parameters of lung perfusion [28] and right ventricular performance [29] can be non-invasively assessed by CT imaging.

Recent developments in MR technology, such as sensitivity encoding (SENSE) and simultaneous magnetization of spatial harmonics (SMASH) imaging, enable two- to threefold reduction in imaging time without any or any significant loss in spatial resolution [30, 31]. Already, MRI has shown its potential of assessment of functional hemodynamic parameters of the pulmonary circulation in general [32] and in patients with CTEPH [33]. These examinations are performed within 15 min and can be evaluated within 30 min.

Conclusion

Both imaging modalities, ce MRA and CTA, revealed equivalent results in visualization of patent pulmonary

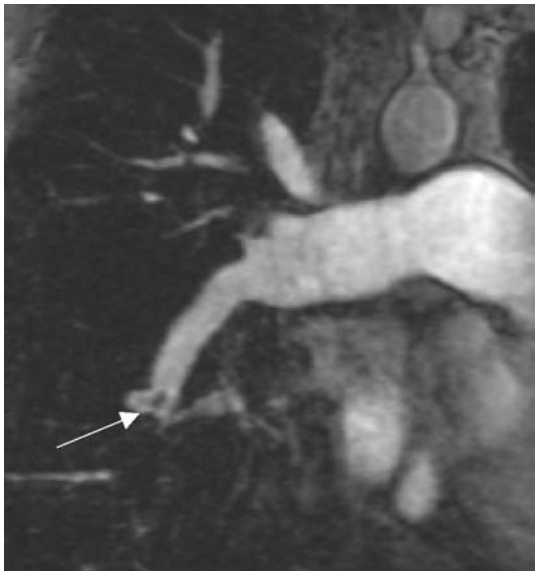

Fig. 4 Demonstration of intraluminal webs (*arrows*) in an MPR of MRA

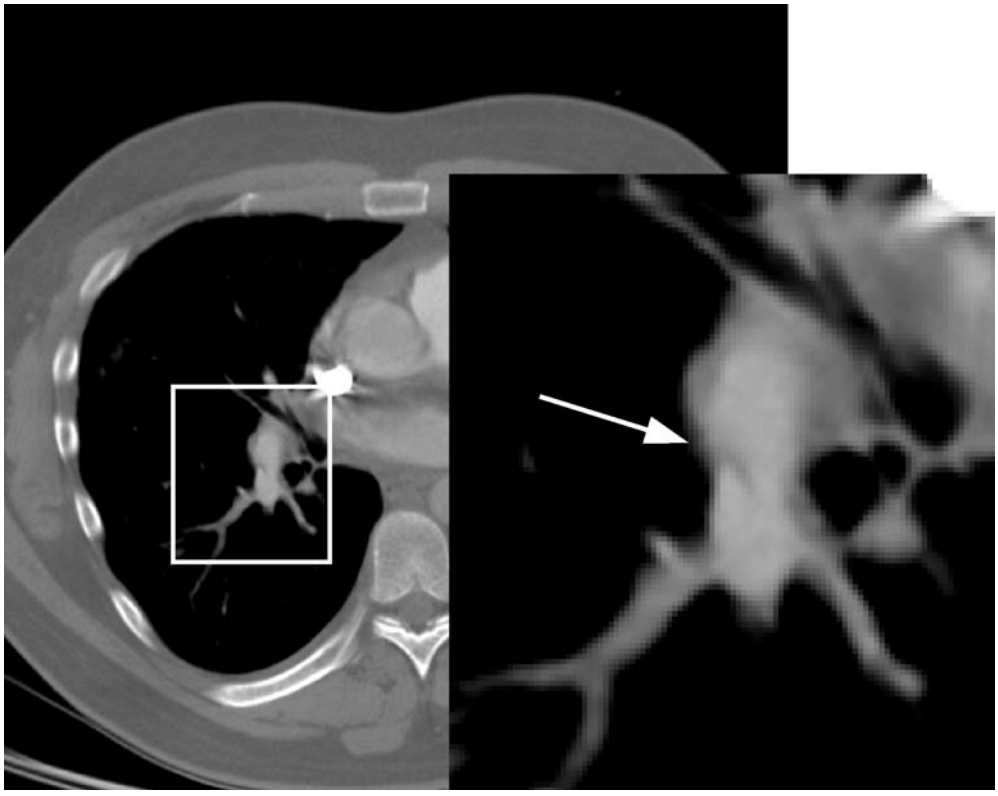

Fig. 5 Demonstration of intraluminal webs (*arrow*) on axial CTA slices

arteries down to the segmental level in patients with CTEPH. Furthermore, both modalities enable an accurate assessment of surgical operability. CTA is superior in visualization of patent subsegmental arteries, direct thrombus load, and intraluminal webs (Figs. 4, 5), whereas ce MRA is better in evaluating abnormal proximal to distal tapering. This reveals an equal diagnostic performance of ce MRA and CTA in terms of characterizing the disease morphologically. The prediction of surgical indication and success additionally, however, depend on hemodynamic parameters. Since MRI has the potential to provide these data non-invasively, MRI could be considered the comprehensive first-line modality in CTEPH patients before and after surgery.

References

1. Frazier AA, Galvin JR, Franks TJ, Rosado-de-Christenson ML (2000) From the archives of the AFIP. Pulmonary vasculature: hypertension and infarction. Radiographics 20:491–524
2. Jamieson SW, Kapelanski DP (2000) Pulmonary endarterectomy. Curr Probl Surg 37:165–252
3. Iversen S, Hake U, Oelert H (1991) Chronic pulmonary embolie. Clinics, diagnostics, and possibilities of surgical intervention. Dtsch Arztebl 88:2836–2844
4. Iversen S, Mayer E, Oelert H (1994) Thromboendarterectomy for thromboembolic pulmonary hypertension. Ann Cardiac Surg 7:170–175
5. Pitton MB, Düber C, Mayer E, Thelen M (1996) Hemodynamic effects of nonionic contrast bolus injection and oxygen inhalation during pulmonary angiography in patients with chronic major-vessel thromboembolic pulmonary hypertension. Circulation 94:2485–2491
6. Roberts HC, Kauczor H-U, Schweden F, Thelen M (1997) Spiral CT of pulmonary hypertension and chronic thromboembolism. J Thorac Imaging 12:118–127
7. Schwickert HC, Schweden F, Schild HH, Piepenburg R, Düber C, Kauczor H-U, Renner C, Iversen S, Thelen M (1994) Pulmonary arteries and lung parenchyma in chronic pulmonary embolism: preoperative and postoperative CT findings. Radiology 191:351–357
8. Kreitner K-F, Ley S, Kauczor H-U, Kalden P, Pitton MB, Mayer E, Laub G, Thelen M (2000) Assessment of chronic thromboembolic pulmonary hypertension by three-dimensional contrast-enhanced MR angiography: comparison with selective intraarterial DSA. Rofo Fortschr Geb Rontgenstr Neuen Bildgeb Verfahr 172:1-6
9. Lotz J, Meier C, Leppert A, Galanski M (2002) Cardiovascular flow measurement with phase-contrast MR imaging: basic facts and implementation. Radiographics 22:651–671

10. Rominger MB, Bachmann GF, Pabst W, Rau WS (1999) Right ventricular volumes and ejection fraction with fast cine MR imaging in breath-hold technique: applicability, normal values from 52 volunteers, and evaluation of 325 adult cardiac patients. J Magn Reson Imaging 10:908–918
11. Kopka L, Vosshenrich R, Muller D, Fischer U, Rodenwaldt J, Grabbe E (1997) Ergebnisse einer Kontrastmittel-gestützten 3D MR-Angiographie in Atemstillstand nach Optimierung des Kontrastmittelbolus. Rofo Fortschr Geb Rontgenstr Neuen Bildgeb Verfahr 166:290–295
12. Kreitner K-F, Kunz RP, Kalden P, Kauczor H-U, Schmitt S, Kuroczynski W, Mohr-Kahaly S, Vogtländer T, Krummenauer F, Laub G, Thelen M (2001) Contrast-enhanced three-dimensional MR angiography of the thoracic aorta: experience after 118 examinations with a standard dose contrast administration and different injection protocols. Eur Radiol 11:1355–1363
13. Kauczor H-U, Heussel CP, Thelen M (1999) Update on diagnostic strategies of pulmonary embolism. Eur Radiol 9:262–275
14. Moser KM, Auger WR, Fedullo PF (1990) Chronic major-vessel thromboembolic pulmonary hypertension. Circulation 81:1735–1743
15. Remy-Jardin M, Remy J, Wattinne L, Giraud F (1992) Central pulmonary thromboembolism: diagnosis with spiral volumetric CT with the single-breath-hold technique: comparison with pulmonary angiography. Radiology 185:381–387
16. Rich S, Levitsky S, Brundage BH (1988) Pulmonary hypertension from chronic pulmonary thromboembolism. Ann Intern Med 108:425–434
17. Tardivon AA, Musset D, Maitre S, Brenot F, Dartevelle P, Simonneau G, Labrune M (1993) Role of CT in chronic pulmonary embolism: comparison with pulmonary angiography. J Comput Assist Tomogr 17:345–351
18. Remy-Jardin M, Remy J, Deschildre F, Artaud D, Beregi JP, Hossein-Foucher C, Marchandise X, Duhamel A (1996) Diagnosis of pulmonary embolism with spiral CT: comparison with pulmonary angiography and scintigraphy. Radiology 200:699–706
19. Schoepf UJ, Kessler MA, Rieger C, Bohme E, Schaller S, Ohnesorge BM, Niethammer M, Becker CR, Reiser MF (2001) Diagnosis of pulmonary embolism with multislice spiral CT. Radiologe 41:248–255
20. Schwickert H, Schweden F, Schild H, Düber C, Iversen S (1993) Detection of chronic recurrent pulmonary emboli using spiral-CT. Rofo Fortschr Geb Rontgenstr Neuen Bildgeb Verfahr 158:308–313 [in German]
21. Gupta A, Frazer CK, Ferguson JM, Kumar AB, Davis SJ, Fallon MJ, Morris IT, Drury PJ, Cala LA (1999) Acute pulmonary embolism: diagnosis with MR angiography. Radiology 210:353–359
22. Meaney JFM, Weg JG, Chenevert TL, Stafford-Johnson D, Hamilton BH, Prince MR (1997) Diagnosis of pulmonary embolism with magnetic resonance angiography. N Engl J Med 336:1422–1427
23. Oudkerk M, van Beek EJ, Wielopolski P, van Ooijen PM, Brouwers-Kuyper EM, Bongaerts AH, Berghout A (2002) Comparison of contrast-enhanced magnetic resonance angiography and conventional pulmonary angiography for the diagnosis of pulmonary embolism: a prospective study. Lancet 359:1643–1647
24. Goyen M, Laub G, Ladd ME, Debatin JF, Barkhausen J, Truemmler KH, Bosk S, Ruehm SG (2001) Dynamic 3D MR angiography of the pulmonary arteries in under four seconds. J Magn Reson Imaging 13:372–377
25. Maki JH, Prince MR, Chenevert TC (1998) Optimizing three-dimensional gadolinium-enhanced magnetic resonance angiography. Invest Radiol 33:528–537
26. Pitton MB, Kemmerich G, Herber S, Schweden F, Mayer E, Thelen M (2002) Chronic thromboembolic pulmonary hypertension: diagnostic impact of multislice-CT and selective pulmonary DSA. Rofo Fortschr Geb Rontgenstr Neuen Bildgeb Verfahr 174:474–479 [in German]
27. Schoepf UJ, Kessler MA, Rieger CT, Herzog P, Klotz E, Wiesgigl S, Becker CR, Exarhos DN, Reiser MF (2001) Multislice CT imaging of pulmonary embolism. Eur Radiol 11:2278–2286
28. Wildberger JE, Niethammer MU, Klotz E, Schaller S, Wein BB, Günther RW (2001) Multi-slice CT for visualization of pulmonary embolism using perfusion weighted color maps. Rofo Fortschr Geb Rontgenstr Neuen Bildgeb Verfahr 173:289–294
29. Wintersperger BJ, Stäbler A, Seemann M, Holzknecht N, Helmberger T, Fink U, Reiser MF (1999) Evaluation of right ventricular performance in patients with acute pulmonary embolism by helical CT. Rofo Fortschr Geb Rontgenstr Neuen Bildgeb Verfahr 170:542–549
30. Reid AW, Roditi G, Lawton T, Kassner AP, Weiger M, Pruessmann KP (2000) Four-dimensional contrast-enhanced MR angiography of the abdominal aorta using sensitivity encoding. Radiology 217:547
31. Sodickson DK, McKenzie CA, Li W, Wolff S, Manning WJ, Edelman RR (2000) Contrast-enhanced 3D MR angiography with simultaneous acquisition of spatial harmonics: a pilot study. Radiology 217:284–289
32. Kreitner K-F, Ley S, Kalden P, Mayer E, Laub G, Thelen M (1999) Assessment of hemodynamic changes in patients with chronic thromboembolic pulmonary hypertension after thromboendarterectomy by breath-hold MR techniques. Eur Radiol 9 (Suppl):312
33. Ley S, Kreitner K-F, Morgenstern I, Thelen M, Kauczor H-U (2002) Bronchopulmonary shunts in patients with chronic thromboembolic pulmonary hypertension: evaluation by helical CT and MR imaging. Am J Roentgenol 179:1209–1215